HHS Public Access

Author manuscript

Acta Biomater. Author manuscript; available in PMC 2020 August 01.

Published in final edited form as:

Acta Biomater. 2019 August ; 94: 306–319. doi:10.1016/j.actbio.2019.02.052.

Film Interface for Drug Testing for Delivery to Cells in Culture and in the Brain★

Min D. Tang-Schomer[1,2,*], **David L. Kaplan**[3], and **Michael Whalen**[4]

[1]The Jackson Laboratory for Genomic Medicine, Farmington, Connecticut 06032, USA. Min.Tang-Schomer@jax.org

[2]University of Connecticut Health Center & Connecticut Children's Medical Center, Department of Pediatrics, Farmington, Connecticut 06032, USA. mtangschomer@uchc.edu

[3]Tufts University, Department of Biomedical Engineering, Medford, MA 02155. David.Kaplan@tufts.edu

[4]Harvard Medical School, Acute Brain Injury Research Laboratory, Massachusetts General Hospital for Children, Charlestown, MA 02129. mwhalen@mgh.harvard.edu

Abstract

Brain access remains a major challenge in drug testing. The nearly 'impermeable' blood-brain-barrier (BBB) prevents most drugs from gaining access to brain cells via systematic intravenous (IV) injection. In this study, silk fibroin films were used as drug carrier as well as cell culture substrate to simulate the *in vivo* interface between drug reservoir and brain cells for testing drug delivery in the brain. In *in vitro* studies, film-released arabinofuranosyl cytidine (AraC), a mitotic inhibitor, selectively killed glial cells in film-supported mixed neural cell cultures; with widened dosage windows for drug efficacy and tolerance compared to drugs in solution. In the brain, the presence of silk films was well tolerated with no signs of acute neuroinflammation, cell death, or altered brain function. Topical application of silk films on the cortical surface delivered Evans blue, a BBB-impenetrable fluorescent marker, through the intact dura matter into the parenchyma of the ipsilateral hemisphere as deep as the hippocampal region, but not the contralateral hemisphere. In a mouse traumatic brain injury (TBI) model, necrosis markers by film delivery accessed more cells in the lesion *core* than by con-current IV delivery; whereas the total coverage including the peri-lesional area appeared to be comparable between the two routes. The complementary distribution patterns of co-delivered markers provided direct evidence of the partial confinement of either route's access to brain cells by a restrictive zone near the lesion border. Finally, film-delivered necrostatin-1 reduced overall cell necrosis by approximately 40% in the TBI model. These findings from representative small molecules of delivery route-dependent

★Part of the Cell and Tissue Biofabrication Special Issue, edited by Professors Guohao Dai and Kaiming Ye.

*Corresponding author.

Disclosure

The authors disclose no competing financial interests.

drug access are broadly applicable for evaluating drug actions both *in vitro* and *in vivo*. Combined with its demonstrated role of supporting neuron-electrode interfaces, the film system can be further developed for testing a range of neuromodulation approaches (i.e., drug delivery, electrical stimulation, cell graft) in the brain.

Graphical Abstract

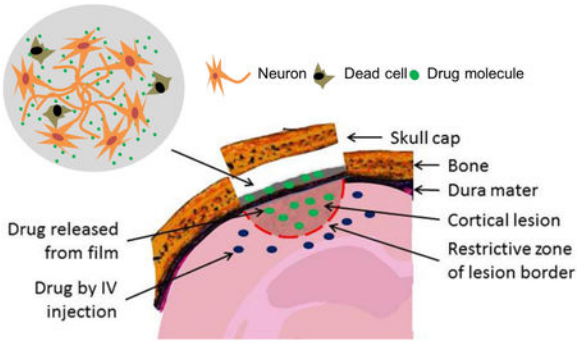

Keywords

Silk; Traumatic brain injury; Drug delivery; Dura; Necrosis; interstitial fluid flow

1. INTRODUCTION

The brain is possibly the most difficult organ to access. The ‘impermeable’ blood-brain-barrier (BBB) prevents most drugs from reaching brain cells via systematic delivery, such as intravenous (IV) injection. Intracranial injection via spinal tap is currently the only direct route to deliver biologicals into the brain, bypassing the BBB. These delivery routes (IV, CSF) suggest indirect exposure of brain cells to most pharmaceutical interventions, requiring transport of drugs through the brain parenchyma. In contrast, *in vitro* cell culture-based preclinical testing for the nervous system relies on direct access of neural cells to test compounds. The high attrition rate of >90% CNS drugs from preclinical testing to clinical trials suggests that drug delivery in the brain needs to be addressed in alternative modes and as early as possible in a drug discovery program [1]. However, the limitations with experimental options using live brain samples have hampered these efforts. Recently, advanced tissue engineering approaches has generated 3D brain-mimetic tissue models that can be used to recapitulate brain functions in terms of basic physiology and in response to mechanical injury [2]. However, these *in vitro* brain tissue models differ from actual brain systems with regard to drug transport, due to the absence of a BBB in the *in vitro* tissue model. Given the significant differences with the *in vitro* versus *in vivo* systems for brain research, it is desirable to be able to directly compare outcomes of interventions in both systems. To this end, we have been exploring a multifunctional material that can interface *in vitro* neural cell cultures and the brain and allow for functional testing of therapeutic interventions. We have envisioned that such a material would support *in vitro* testing of biologicals and also provide an option to be used as brain implants for evaluating *in vivo* drug actions. As a first step towards our goal of direct *in vitro*-to-*in vivo* translations, the

interface material between drugs and cells needs to be evaluated for drug access and cell responses in comparison to existing delivery options, in both *in vitro* and *in vivo* systems.

As a brain implant, materials need appropriate mechanical stiffness to match the brain while maintaining function to deliver biologics or a stimulus. For example, the elastic modulus of a typical silicon-based electrode probe is near 100 Gpa, approximately six orders of magnitude higher than the stiffness of brain tissue which is around 100 kPa and similar to Jell-O [3]. The mismatch of stiffness at the tissue-material interface results in interfacial strains during the lifetime of the material implant that can lead to brain tissue damage and a reduction in function of the implant. Polymer materials such as silk fibroin films have been used to coat electrode probes to mediate this mechanical discrepancy between the brain tissue and the implant device [4]. The flexible silk fibroin film can also be grafted onto the brain surface and the optical clarity allows for careful placement on specific cortical regions [5]. In pre-clinical animal studies, once the silk fibroin film was grafted onto the mouse brain it stayed in place and caused no adverse inflammatory responses in the host animal [6].

When used as a substrate for *in vitro* cell culture, the silk fibroin films showed excellent compatibility with primary neurons of the brain and the peripheral nervous system [6,7]. For functional modulation, silk fibroin films can deliver electrical signals to neuronal cultures through embedded electrodes [6,8]. Due to the aqueous processing used in the preparation of these silk-based materials [9,10], silk fibroin is amenable to chemical and biological functionalization to deliver therapeutics, including growth factors, nucleic acids and antibodies with sustained release [11]. The release kinetics from the films are controlled by film processing, including thickness, porosity, chemical functionalization and crystallinity [12], and can be modeled as a function of molecular weights of entrapped analytes [13]. These studies have established silk fibroin films as a promising material platform for *in vitro* and *ex vivo* device development with the goal of promoting neural regeneration and functional neuromodulation. Silk fibroin polymer-based systems have also been used as brain implants to deliver a small molecule, adenosine, for seizure control in rat epilepsy models [14–16]. In these studies, a combination of drug-loaded microspheres and encapsulating films were used in order to maximize the drug loading dose and to control the small molecule's release kinetics [16]. In addition, their specific research questions required deep brain implantation of a tissue-displacing scaffold [15]. Nevertheless, the promising drug effects in epilepsy control suggest that the silk fibroin-based system may be adapted for drug testing for the brain for broad applications.

In this study, silk fibroin films as an interfacial material were used to evaluate drug actions in comparison to conventional drug delivery approaches in *in vitro* neuronal cultures (i.e., film vs. solution delivery) as well as *in vivo* brain injury studies (i.e., film vs. IV injection). We anticipated that once the film processing was optimized for drug delivery to neuronal cultures *in vitro*, similarly fabricated films could be grafted onto brain lesions to directly evaluate drug actions in a live brain. This capability would be desirable to screen drugs that target specific regions of the brain and/or cell types. The film-based interface material addresses our needs in two aspects. First, brain cells growing on the film would respond similarly to film-bound drug molecules as the cortical cells in direct contact of a drug-loaded film implant; therefore, the outcomes in both *in vitro* and *in vivo* systems would be

comparable. Secondly, in both systems, drugs are released from a film carrier with similar release kinetics. Compared to the intravenous injection route, the *in vivo* film-based delivery would not be affected by the significant distance the drug must travel in the blood stream, the BBB and access to a particular cortical region.

For the *in vitro* study, we compared the action of an anti-mitotic drug, arabinofuranosyl cytidine (AraC), for killing glial cells in primary cortical cell cultures on drug-embedded films versus drugs in solution. Instead of designing a brain tumor model to test AraC's anti-tumoral action *in vivo*, which ideally would require a superficial location of the cortex for a film's easy access, we focused on examining actions of small molecules with similar sizes and polarity as AraC for *in vivo* film-delivery studies. We took advantage of a direct route to access a brain cortical lesion in traumatic brain injuries (TBI) that necessitate surgical removal of the skull (craniotomy). We assessed film delivery of fluorescent small molecular markers in a mouse controlled cortical impact (CCI) injury model for which acute cell injury and uptake of these markers have been characterized in previous studies [17]. We first examined film-based delivery in an intact brain of a BBB-impermeable fluorescent dye, Evans blue, to assess drug penetration across the dura mater (the outermost membrane covering the cortex); as well as the brain's cellular and functional responses to the presence of the silk film implant. By comparing co-current delivery by film versus IV injection of different cell necrosis markers in a same brain injury model, we identified limitations of either delivery route with regard to small molecule drug access in the brain lesion. Finally, we assessed neuroprotection by film delivery of necrostatin-1, an anti-inflammatory drug previously shown to reduce cell necrosis after brain injury[18], to demonstrate the feasibility of the silk film delivery approach for preclinical drug testing. Together, these studies showed that silk fibroin films can be used to efficiently evaluate drug actions both *in vitro* and *in vivo*. This approach can be further adapted to efficiently screen drugs targeting specific brain regions and/or cell types such as focal lesions and brain tumors.

Methods

1.1. Silk fibroin films

Silk films have been routinely produced in our laboratories for a wide range of biomedical applications including *in vitro* cultures of mammalian cells [6,7,19,20] with standardized processes that ensures purity and consistency [21]. Briefly, cocoons of *B. mori* silkworm (Tajima Shoji Co., Yokohama, Japan) were boiled for 20 min in 0.02 M Na_2CO_3 and rinsed to extract the glue-like sericin from the structural fibroin proteins [22]. The fibroin extract was dissolved in a 9.3 M LiBr solution at 60°C for 4–6 h and then dialyzed in distilled water using Slide-a-Lyzer dialysis cassettes (Pierce, MWCO 3,500) for 2 days. After centrifugation (13,000 g, 20 min) to remove insoluble residues, a 5–8% (wt/vol) silk fibroin solution was obtained and stored at 4°C. Silk films were produced by casting sterile-filtered silk fibroin solution onto polydimethylsiloxane (PDMS) molds (14 mm dia., 0.5–1 mm thick), or directly cast in polystyrene culture plates (65 μl/cm^2) and drying in a fume hood overnight. The films were rendered water-insoluble by β-sheet formation via water annealing in a water-filled desiccator for 45 min.

1.2. Drug-loaded silk films for *in vitro* cell culture

For *in vitro* studies, arabinofuranosyl cytidine (AraC) (Sigma-Aldrich, St. Louis, MO, USA) was mixed in 1% silk fibroin solutions, and directly cast in a 96-well polystyrene culture plate (25 μl/well; i.e., ~70 μl/cm^2 or ~7 μg/mm^2 or 250 μg/film silk fibroin). The films were dried at 60°C for 2 hrs. Once dry, the films were water annealed in a water-filled desiccator for 45 minutes to induce β-sheet formation[9,10], and then left to dry again in a tissue culture hood. AraC- encapsulated films were coated with polylysine solution (Sigma, 0.1 mg/mL) for 2 hours, washed once with saline and let dry before cell plating. Drug amounts in films were calculated as the initial amount loaded in the dry film subtracting losses during polylysine coating and wash that were measured with a spectrophotometer SpectraMax M2™ (Molecular Devices Corp., Sunnyvale, CA, USA) of absorbance at 272 nm. Drug concentrations were expressed as the total amount (in moles) of AraC loaded in the film per unit volume of the final culture media; the media remained unchanged throughout 10-day culture. For control bath cultures, AraC of corresponding concentrations in solution was applied to the media at day 2 *in vitro* (DIV2). Drug concentrations represented the retaining amount in the films after processing. For each condition per time-point of examination, three identical cultures were prepared.

1.3. Drug-loaded silk films for brain implantation

For *in vivo* studies, the drugs were mixed into a final 2% (w/v) silk fibroin solution and casted onto 4 mm dia. polydimethylsiloxane (PDMS) molds (Sylgard 184; Dow Corning, Midland, MI, USA) at 13 μl/piece (~7 μg/mm^2 or 260 μg silk fibroin). The film weight and dimension were determined in pilot studies for best conformal contact with the brain cortex and sufficient small molecule drug loading. The films were then left in a tissue culture hood to dry at room temperature. Once dry, the films were water annealed in a water-filled desiccator for 45 minutes to induce β-sheet formation, and then left to dry again in a tissue culture hood. Once dry, the films were carefully lifted off the surface of the PDMS molds with #10 scalpel and forceps, being careful to avoid cracking the film. Films were storedin Parafilm-wrapped tissue culture petri dishes at 4°C until use.

Evans blue (molecular weight M.W., 961 Daltons), propidium iodide (M.W., 668) and Hoechst 33258 (M.W., 534) were from Sigma, YOYO-1 (M.W., 1,271) was from Invitrogen. Necrostatin 3-FITC and necrostatin-1 (5-[(7-chloro-1H-indol-3-yl)methyl]-3-methyl- 2,4-imidazolidinedione) (M.W., 261) [23] were gifts from Dr. Whalen's laboratory. For each film implant, drug amounts were: Evans blue (0.26 mg or 0.27 μmol), propidium iodide (2.5 μg or 3.75 nmol), YOYO-1 (4.8 μg or 3.75 nmol), Hoechst 33258 (2 μg or 3.75 nmol), necrostatin-1 & 3 (2 μg or 8 nmol). Pilot studies determined the maximum loading quantity of Evans blue at ~0.3 mg to yield an intact silk film; and the propidium iodide loading quantity for consistent labelling of necrotic cells in injured animals. YOYO-1 and Hoechst 33258 loading were controlled to achieve the same moles per film as propidium iodide for comparative studies. Necrostatin loading dose was scaled from 24 nmol used by a previous study with intraventricular injection in the controlled cortical impact mouse model, in which this dose was found to reduce acute cell injury [18].

For each drug/film implant, the numbers of animals used were: Evans blue (n > 20), propidium iodide (n = 15; three for sham, four for pre-injury, four for 1 hr post-injury, four for 5 hr post-injury applications), Hoechst plus propidium iodide (n = 3), necrostatin-3-FITC (n = 3; in 4% methyl-β-cyclodextrin in PBS), necrostatin-1 (n = 5; in 4% methyl-β-cyclodextrin in PBS). Equal numbers of vehicle films (4% methyl-β-cyclodextrin in PBS for necrostatin −1 & −3 and PBS for other small molecules) as drug-loaded films were used per experimental group.

For PI and YOYO-1 comparative studies, three animals per group were used: vehicle film plus PI/YOYO-1 injection, PI film-only plus YOYO-1 injection, YOYO-1 film-only plus PI injection, PI/YOYO-1 film.

1.4. Primary cortical cell isolation and culture

The brain tissue isolation protocol was approved by Tufts University Institutional Animal Care and Use Committee and complies with the NIH Guide for the Care and Use of Laboratory Animals. Primary rat cortical neural cell culture was prepared as previously reported [24]. Briefly, cortices from embryonic day 18 (E18) Sprague Dawley rats (Charles River, Wilmington, MA, USA) were isolated, dissociated with trypsin (0.3%, Sigma) and DNase (0.2%, Roche Applied Science, Indianapolis, IN, USA) followed with trypsin inhibition with soybean proteins (1 mg/mL, Sigma), centrifuged, and plated at 200–625,000 cells/cm^2 in NeuroBasal media (Invitrogen, Carlsbad, CA, USA) supplemented with B-27neural supplement, penicillin/streptomycin (100 U/ml and 100 μg/ml), and GlutaMax™ (2mM) (Invitrogen). Cultures were maintained in 37°C, 100% humidity and 5% CO_2 in an incubator (Forma Scientific, Marietta, OH, USA) for up to 16 days *in vitro* (DIV 1–16).

1.5. Cell viability assay

Cell viability was assessed using the LIVE/DEAD Viability Assay Kit (Invitrogen). Briefly, culture media was replaced with Dulbecco's phosphate-buffered saline (DPBS; Invitrogen) containing calcein AM (4 μM) and ethidium homodimer-1 (2 μM). After 30 minutes incubation at 37°C, the cells were changed into fresh culture media, and viewed under a fluorescence microscope (Leica DM IL; Leica Microsystems, Wetzlar, Germany) equipped with a digital camera (Leica DFC340 FX). Fluorescence images were acquired using excitation at 470±20 nm and emission at 525 ±25 nm for live cells, and excitation at 560 ± 20 nm and emission at 645 ±40 nm for dead cells, respectively. NIH ImageJ software was used to quantify cell numbers.

1.6. Immunocytochemistry of *in vitro* neural cell cultures and image analysis

Cells were fixed with 4% paraformaldehyde (Fisher Scientific, Pittsburgh, PA, USA) for 20 min, washed, permeabilized with 0.1% Triton X-100 (Fisher Scientific) including 4% goat serum (Sigma) for 20 min, followed with incubation of primary antibodies overnight at 4°C. After three 10 min washes, cells were incubated with secondary antibodies for 1hr at room temperature, followed by extensive washes. Antibodies included: anti-glial fibrillary acidic protein (GFAP, mouse, 1:1000; rabbit, 1:500; Sigma), anti-βIII-tubulin (b3TB, rabbit, 1:500; Sigma), anti-Iba1 (Iba1, mouse, 1:250; Sigma), goat anti-mouse or rabbit Alexa 488 and 568 (1:250; Invitrogen) secondary antibodies. Fluorescence images were acquired on a Leica

DM IL fluorescence microscope with excitation at 470±20 nm and emission at 525±25 nm for Alexa 488, and excitation at 560±20 nm and emission at 645 ±40 nm for Alexa 568.

1.7. Silk film implantation onto mouse brain surfaces.

The implantation and the trauma protocol were approved by the Massachusetts General Hospital Institutional Animal Care and Use Committee and complied with the NIH Guide for the Care and Use of Laboratory Animals (IACUC# 2005n000286). Mice (CL7/BL6, 3 months of age, Jackson Laboratories, Bar Harbor, ME) were anesthetized with 4% isoflurane, 70% N_2O and balance $O_2$and positioned in a stereotaxic frame. Blow by anesthesia was maintained via a nose opening in the tubing leading from the anesthesia box and isoflurane was titrated to quiet respirations and lack of toe pinch response at a level that avoids hypotension [25]. A 5-mm craniotomy was made using a portable drill and trephine over the left parietotemporal cortex (the center of the coordinates of craniotomy relative to bregma: 1.5 mm posterior, 2.5 mm lateral), and the bone flap was removed (craniotomy). A 4-mm diameter silk film was placed on top of the exposed brain surface within the burr hole opening. The craniotomy was replaced and the scalp was sutured closed. Mice returned to their cages to recover from anesthesia.

1.8. Controlled cortical impact (CCI) model of brain trauma and systemic administration of cell necrosis markers

The mouse controlled cortical impact (CCI) model and the method of cell necrosis marker, propidium iodide and YOYO-1, administration for assessing acute cell injury were described previously [18,25]. Briefly, after craniotomy, controlled cortical impact is produced using a pneumatic cylinder with a 3-mm flat-tip impounder, velocity 6 m/s, and impact depth of 0.3 mm. After CCI, the scalp was sutured closed, anesthesia was discontinued, and mice allowed to recover in room air in their cages. Sham injury involved craniotomy but no cortical impact. At 30 min before sacrificing the animal, propidium iodide (250 mg/ml in PBS; 25 mg or 40 μmol per animal) or YOYO-1 (1:10 dilution in PBS of stock 1 mM in DMSO; or 10 nmol per animal) or combined was administered by intraperitoneal injection and/or tail vein IV injection in a total volume of 100 μL.

1.9. Assessment of small molecule release from silk film implants into the brain

Mice were deeply anesthetized with isoflurane and decapitated, and brains were removed and frozen in liquid nitrogen vapor. Coronal sections (14 μm) were collected (200–250 μm apart) from the anterior to the posterior brain, mounted on poly-L-lysine-coated slides and stored at −80°C. Fluorescence images of Evans blue uptake were acquired on a Leica DM IL fluorescence microscope with excitation at 540 nm and emission at 680 nm.

1.10. Assessment of cell necrosis and apoptosis

Regions of interest for cell counts in the contused cortex were selected based on previous reports showing robust cell necrosis in perilesional cortex in the CCI model [25]. Cortical regions of interest were 200× microscopic fields (638×479 μm) at the medial and lateral edges of the contusion, and one cortical field directly under the impact site. Using a fluorescence microscope (as above), propidium iodide-positive cells were counted in a total

of three brain sections located within the center of the contusion and separated by at least 250 μm, for a total of nine 200× cortical fields assessed per animal. For studies specifying 400x cortical fields, three non-overlapping fields in the lesion core were imaged per section for a total of three sections per brain. Cell count data for each mouse were the average of cortical brain fields.

Cell apoptosis was assessed with a TUNEL assay kit (Invitrogen) that uses terminal deoxynucleotidyl transferase to catalyze the incorporation of luorescein-12-dUTP at the free 3'-hydroxyl ends of the fragmented DNA in apoptotic cells. Cells with fluorescein-labeled DNA were imaged with fluorescence microscopy with Ex/Em 488/520 nm.

1.11. Morris Water Maze test for spatial memory

Spatial memory acquisition was assessed using the Morris Water Maze (MWM) testing using five hidden platform trials, as previously described on postinjury days 8–9 [25]. A probe trial (60 s) is used to assess hippocampal dependent spatial memory retention [26]. A white pool (83 cm diameter, 60 cm deep) was filled with water to 29 cm depth. A round, clear plexiglass platform 10 cm in diameter was positioned 1 cm below the surface of the water approximately 10 cm from the southwest quadrant. For each trial, mice were randomized to one of four starting locations (north, south, east, west) and placed in the pool facing the wall. Mice were given a maximum of 90 seconds to find and mount the invisible platform. If the mouse failed to reach the platform by 90 seconds, it was placed on the platform by the experimenter and allowed to remain there for 10 seconds. Mice were dried and kept warm under heat lamps between trials. Performance in the MWM was quantitated by latency to the platform. Following five hidden platform trials a probe trial was done in which mice were placed in the tank with the platform removed and latency in the target quadrant was measured (60 s maximum). Four animals per group were used.

1.12. Statistical analysis

Data are mean± standard error of mean (S.E.M.). Student's t-test was used for cell count data. Morris Water Maze test data (platform acquisition latencies) were analyzed by two-factor repeated measures analysis of variance (group-time). For all tests, $p < 0.05$ was considered significant.

2. Results

2.1. Silk film-based delivery of anti-mitotic drug to primary cortical cell cultures for purification of neurons

To assess the *in vitro* function of silk film-based drug delivery, arabinofuranosyl cytidine (AraC, M.W., 243.22), an anti-mitotic drug used to purify neuron cultures *in vitro* [27]and a cancer chemotherapeutic agent [28,29]were selected. For a typical primary neural cell culture, AraC is applied in the culture media at <4 μM for no more than 48 hours; higher dosages or longer durations are toxic to neurons. To examine drug effects over a prolonged period of time, we compared cultures of primary cortical cells on drug-loaded films with those applied with drugs in solution at corresponding concentrations (0.25 – 64 μM AraC expressed as the final amount released per unit volume of the culture media, see Methods).

Figure 1 A–C provide the release kinetics of AraC-silk films. The comparison of recovered AraC doses after dissolving silk films in LiBr to the original loading doses indicates that films contained ~100% of the calculated loading dose of the drugs (Fig. 1A). There was a burst release of AraC that was proportionate to the initial loading dose during the poly-L-lysine coating step (Fig. 1B); this initial drug loss was subtracted to reflect the actual amount of drug in the films when compared with solution controls. Post-processed AraC-silk films exhibited rapid release within the first 2 hr and slower release up to day 7 *in vitro* (Fig. 1C). Figure 1D shows scanning electron microscopic (SEM) images of silk films. The fractured cross-section was ~5 μm thick (Fig. 1D–a) and the film surface was smooth (Fig. 1D–b).

The efficacy of AraC in reducing glial cell numbers was determined by co-staining cultures at DIV 10 for GFAP and β III tubulin (b3TB) (Figure 2A, B). Untreated cultures in control plates or using films without drugs had ~41 GFAP-positive glial cells per 100× field of view (1.22 cm^2) (Fig. 2A, *green*). AraC in solution eradicated glial cells at concentrations of 0.5 – 1 μM, and was highly toxic to neurons at > 4 μM. The 4 μM concentration produced fewer neurons that did not form robust networks characteristic of healthy neuronal cultures (Fig. 2B). In comparison, AraC in films reduced glial cells to ~7 cells at concentrations of 0.25 μM to 8 μM, and to ~2 cells (per 100× field of view) at 16 μM while leaving most of the neuronal networks intact (Fig. 2B). These data showed that the film as drug carrier had a wider dose window for drug efficacy than solution. In addition, within the effective dose range (0.5–8 μM), there appeared to be dose-independence of AraC-loaded films for drug efficacy.

Drug toxicity was assessed by cell viability assay at 24 hr exposure (DIV1) and DIV10 (Fig. 2C), quantified as live cell percentage (calcein AM stained positive cells over DAPI stained total cell numbers, see Methods). AraC in solution at doses > 8 μM lowered cell viability to ~10% at 24 hours, and to <5% at DIV10. At ≥ 16 μM most of the cells were dead by DIV10. In comparison, cultures with AraC in films retained viability of ~35% at 24 hours, with modest reduction to ~21% at DIV10 at concentrations as high as 32 μM. Exposure time had a strong effect on drugs in solution, but a much milder effect on film-bound drugs. For example, AraC in solution showed strong toxicity at DIV 10 compared to 24 hr (red dashed line vs. blue dashed line). However, such difference was not observed in cultures on drug-loaded silk films (red solid line vs. blue solid line) of low concentrations (<4 μM), and the reduction in cell viability was modest at high concentrations (8–32 μM). Overall, cells showed a wider window of dose tolerance on drug-loaded films than to drugs in solution.

2.2. Silk film-based delivery of small molecules to localized cortical regions

To evaluate silk films as carrier systems for drug delivery in the brain, Evans blue (EB, M.W., 961), a fluorescent small molecule that cannot pass through the blood-brain-barrier (BBB) due to plasma protein binding [30], was assessed (Figure 3). Following craniotomy, films loaded with Evans blue were placed on top of the intact dura mater. EB released from silk film implants was detected in the ipsilateral cortex by 24 hr and the ipsilateral hippocampus by day 3 (Fig. 3A and B). EB was not detected in the contralateral cortex or hippocampus (Fig. 3C and D). The radial diffusion pattern of EB shown in a series of coronial brain sections indicated localized delivery in the cortical area directly beneath the

film, which persisted for >1wk (Fig. 3E and F). Control experiments in which EB solution was placed directly on top of the exposed brain surface resulted in a rapid loss of dye and no brain cell labeling. These data suggest that small molecule drugs can be localized to selective cortical and deep brain regions of intact brain via silk film-based delivery.

2.3. Brain tissue response to the presence of silk films and functional capacity

To determine the brain's response to the presence of silk films, we examined EB film-implanted brain inflammatory responses, cell apoptosis and the host animal's behavioral tests (Figure 4). To assess the acute foreign body response, we harvested mouse brains at day 3 after EB film implantation, sectioned and stained for microglial (Iba1+) and astrocytic (GFAP+) cell markers. The ipsilateral hemisphere showed consistent EB staining but no positive staining for Iba1 nor GFAP (Fig. 4A, a–c, *left*). The contralateral hemisphere was negative for EB, GFAP and Iba1 (Fig. 4A, a–c, right). TUNEL staining detected negative cell apoptosis (Fig. 4B, a-TUNEL only; b-TUNEL overlaid with EB uptake).

We did not observe any behavioral changes of mice with silk films grafted onto intact dura (n>20, no quantification). Nevertheless, we expected some minor cortical gliosis due to possible effects of craniotomy that accidentally damages the dura mater. In our previous study with silk film implants after controlled dura removal (durotomy), we observed that reactive astrocytes in direct contact with the silk film can respond to the film's surface micropattern to present GFAP+ aligned processes [6]. Considering that silk film can be applied onto intact dura or for some applications on brain surfaces without the dura (such as subdural electrocorticography) with the latter being more invasive, we decided to compare brain function in animals with durotomy with or without silk film implants. We used the Morris Water Maze (MWM) testing for spatial learning and memory with hippocampus-dependent (probe test) and -independent aspects (hidden platform acquisition) [26]. To assess potential functional deficit, MWM test was carried out between day 8–9 after EB film implantation. Both the implant group and sham group behaved equally well in finding the hidden platform after repetitive trials (n=4/group, 5 trials per animal over 2 days), indicating no change of the host animal's spatial memory by the silk film's presence in the brain (Fig. 4C). No statistical difference was found between the implant and sham groups for the probe test (Fig. 4D), indicating that neither the silk film presence nor EB release into the cortex had any measurable negative impact on hippocampal function.

2.4. Silk film-based delivery of necrosis cell markers in a mouse traumatic brain injury (TBI) model

To evaluate silk film-based delivery of small molecules in damaged brain, we used a controlled cortical impact (CCI) mouse model and assessed acute cell injury via necrosis marker, a cell impermeant nuclear stain propidium iodide (PI, M.W., 668) (Figure 5). Previous studies have established the time-window for the acute phase of cell injury to be within 6 hr [18]. To capture the acutely injured cell populations within this time window, PI-films were placed on the brain surface immediately after injury and resided in the brain for 1 hr or 5 hr before animal sacrifice (Fig. 5A, schematics). In un-injured animals with PI-film implants ("Sham/PI film"), no PI+ cells were found in the brain (Fig. 5A, a). After injury, PI

+ cells were found in brains with PI films in either 1 hr or 5 hr post-injury groups with no noticeable differences between the two groups (Fig. 5A, b, *red*).

In another set of experiments to evaluate potential non-specific marker absorption, films were loaded with both PI and Hoechst 33258, a cell permeant nuclear stain (Fig. 5A, c). Hoechst was taken up by most of the cortical cells (*blue*), only a subset of Hoechst+ cells were also positive for PI (*pink*). These data indicate that the uptake of makers is driven by cell-specific biology, i.e., Hoechst 33248 for all cells and PI only for injured cells.

We hypothesized that due to the flexibility and conformal contact of the thin silk film to the brain surface, its presence would not interfere with the brain tissue's response to TBI. To examine this, we quantified PI+ cells with film delivery before and after CCI and compared with tail vein injection. The PI-film were either applied to the animal 24 hr before injury (pre-treat) or placed on the contusion site immediately after injury and resided for 5 hrs (post-treat), and compared with those with systemic PI injection (tail IV inj.). IV injection was performed at 1 hr post-injury and allowed 30 min before animal sacrifice: Previous reports have determined that 30 min post-IV is sufficient for brain-wide PI absorption in this animal model [18]. PI+ cells were present not only in the lesion core with obvious tissue damage but also in surrounding peri-lesional region with normal tissue appearance. Therefore, to evaluate PI access to the cortical tissue by different delivery routes, we counted PI+ cells with a relatively low magnification (200x) encompassing large fields of view. PI+ cell counts showed no statistical difference among systemic PI injection (n = 8), PI film pre- (n = 4) or post-treatment (n = 8 of four for 1 hr and four for 5 hr post-injury group) (Fig. 5B).

2.5. Silk film-based delivery compared to systemic delivery to access brain lesion

To compare silk film-based delivery with the systemic delivery route, we used reciprocal delivery of PI and YOYO-1 (M.W. 1,271), an alternative cell impermeant nuclear stain, by silk film and IV injection, in the CCI model (Figure 6). PI and YOYO-1 were loaded in equal mole amounts per film to eliminate dose-dependent diffusion differences. Injured animals were grouped into, 1) vehicle films + IV injection of PI and YOYO-1, 2) PI films + IV injection of YOYO-1, 3) YOYO-1 films + IV injection of PI, and 4) PI/YOYO-1 combined films + IV injection of control saline solution. All films were placed immediately after injury, and resided in the brain for 1.5 hr. IV injection was performed at 1 hr post-injury and allowed 30 min before animal sacrifice (see above). Figure 6A shows representative histological images from brains with both a PI film implant and YOYO-1 IV injection (schematized in a), including the lateral (b), proximal (c), medial (d), and inferior (**e**) edges surrounding the lesion (Inj), and a higher magnification of the lesion core (**f**). YOYO-1 (*green*) via IV injection labeled cells predominately in the periphery of the contusion (near the dotted demarcation in **b** and **d**), and the inferior part of the contusion (opposite to the demarcation in **c**). By contrast, silk film-delivered PI labeled cells throughout the lesion that included YOYO-1-negative cells (*red only*), as well as those co-stained with YOYO-1 (*yellow*). These results showed that there is a peri-lesional restrictive zone that limits access of small molecules via the systematic delivery route.

Figure 6B shows representative fluorescence images of the damaged cortex marked with PI and YOYO-1 (PI, *red*, and YOYO-1, *green*) co-delivery by different routes. There were marked differences in marker distribution. For example, mixed distribution and co-localization were observed for both markers delivered with the same route, either by IV injection (Fig. 6B–a) or by the film implant (Fig. 6B–d). However, when the molecules were delivered via different routes simultaneously, they were preferentially distributed either in the lesion core or the peri-lesional regions, corresponding to film-based vs. systemic delivery respectively (Fig. 6B–b & c). In addition, there was little mixing of the two markers near the lesion border where their access areas converged.

To evaluate marker access to the lesion core, i.e., corresponding to Fig. 6A–f, not including b-e, we counted positively stained cells at a higher magnification (400x) than PI+ cell count in Figure 5, and found delivery route-dependent differences in marker access. Figure 6C shows quantification of PI+ (*red*) and YOYO-1+ (*green*) cell counts in the lesion *core* in all four groups of animals (n = 3 per group). When PI and YOYO-1 were combined in IV injection, or in film delivery, PI+ and YOYO-1+ cell numbers were not significantly different, though YOYO-1+ cells were generally fewer than PI+ cells perhaps due to YOYO-1's twice as big size as PI's. However, when the molecules were delivered via different routes, quantification showed that there were significantly more cells marked with film-delivered markers compared with IV injected markers (PI film/YOYO-1 IV, 96% difference, student's 2-tailed paired t-test, $p = 0.03$; YOYO-1 film/PI IV, 219% difference, $p = 0.002$). These results demonstrated that the film-based delivery accessed the lesion core that had limited access by systemic injection due to the peri-lesional restrictive zone.

Interestingly, the numbers of positive cells stained by either PI or YOYO-1, both film-delivered (last group in the histogram), were significantly lower than when only one marker was film-delivered. This difference suggested competition of the two markers for the uptake of a limited number of necrotic cells. Accordingly, the combined numbers of PI+ and YOYO-1+ cells in the last group were similar to the positive cells by single marker film-delivery.

2.6. Silk film-based delivery of necrostatin for reducing acute cell injury in mouse brain after trauma

We next used this strategy to deliver a small drug, necrostatin-1(Nec1, M.W., 260), to injured cortex in order to reduce acute cellular injury (Figure 7). Necrostatin-1 administered via the intracerebroventricular route was found to reduce acute cellular injury and chronic tissue damage after CCI [18]. For preclinical drug applications, mice were implanted with necrostatin-1 or −3 loaded silk films for 24 hrs before injury, and animals were sacrificed at 5 hr post injury. PI-injection was performed at 30 min before sacrifice. Fluorescently tagged necrostatin 3 (Nec3-FITC) released from silk film implants was taken up by cortical cells in the lesion (Fig. 7A–a), indicating drug access to the injured brain tissue. Mice treated with Nec1-loaded silk films had ~ 40% reduction of PI+ cells compared to vehicle-loaded films in the brain lesion, with 96 ± 8 vs. 164 ± 8 cells per 200 × field of view, respectively (n = 5/per group, student's t-test, $p < 0.01$) (Fig. 7B).

4. Discussion

Silk fibroin films were examined as interfacial biomaterials for the evaluation of drug delivery and cell response in neuronal cultures and the brain. *In vitro*, drug-loaded films selectively killed glial cells by releasing AraC, a mitotic inhibitor, to film-supported mixed neural cultures; and this effect had widened dosage windows for drug efficacy and tolerance compared to AraC in solution. *In vivo*, the silk fibroin films loaded with small molecule markers delivered these into the cortical regions of the brain through the intact dura matter. These studies further showed that film-delivered small molecules can penetrate as deep as the hippocampal region while remaining confined to the ipsilateral hemisphere. In a mouse TBI model, film-delivered necrosis markers accessed injured cells in the lesion core that showed limited drug passage by systemic IV delivery, due to a restrictive zone near the lesion border. However, the total coverage of necrotic cells including those in the peri-lesional area appeared to be comparable between the two different delivery routes. Finally, necrostatin-1 delivered by silk films reduced overall cell necrosis, including both the core and the peri-lesional area, by approximately 40%. Together, these studies demonstrate that the silk fibroin film with on-site application and localized drug delivery is suitable for evaluating drug actions in the whole brain; and this system can enable more efficient comparison with film-based *in vitro* drug studies. The findings with representative small molecules of delivery route-dependent drug access and cell exposure in the brain will be instructive for drug delivery to the brain. Combined with its support of neuronal cultures, these silk fibroin films can evaluate drug actions in both *in vitro* and *in vivo* systems related to the brain more efficiently compared to current options. This alternative approach could be used to facilitate the translation of preclinical drug studies into pharmaceutical interventions for the brain, and should be particularly useful for drugs requiring region and cell type specificity.

4.1. Film as drug carrier and culture substrate for *in vitro* drug testing

The aqueous-based processing of silk films supports the entrapment of a wide range of bio-active reagents, including drugs, enzymes, and antibodies with prolonged stability [11]. These features make silk an excellent biocompatible reservoir for drug delivery. Our data showed that a thin (~5 μm thick, 4 mm dia.) silk fibroin film loaded at least 128 μM small molecule drugs (i.e., AraC). To adapt the silk fibroin films for *in vitro* neuronal cultures, the inert surface needs to be modified to support cell adhesion. Polylysine coating resulted in about a 10–60% drug loss during the washing step; with the loss proportional to the total drug loading dose. This indicated that the silk film is a matrix-based diffusion system: water permeation leads to volume expansion of the bulk polymeric material, causing the release of entrapped drug depending on drug solubility, silk polymer crystallinity and other variables. An initial burst release within the first 2 hours is coincident with silk film swelling during hydration as observed in other studies [31]. The initial burst release of drug is also commonly observed in controlled-release systems for small molecules owing to their low molecular weights[32]. Strategies for controlling polymeric swelling and drug-polymer conjugations can be used to achieve more sustained drug release [33]. In addition, the current silk films are limited in surface coatings, resulting in drug loss during the processing. Thus, alternative modification strategies of the silk films, such as covalent bonding of

polylysine or other cell adhesion peptides [34], or introducing positive charges such as tropoelastin blends [35], can facilitate a reduction of losses of loaded drugs. The versatile biophysics and biochemistry of silk fibroin as a high molecular weight protein amphiphile allows exploration of materials processing and modifications in order to optimize specific drug delivery needs; from loaded drug amounts to sustained release profiles.

Silk film as drug carrier as well as cell culture substrate showed different effects on neural cells than drugs in solution with regards to dose responses for both efficacy and toxicity. The anti-mitotic drug, AraC, is incorporated by cells during cell replication; inducing DNA damage and apoptotic cell death. AraC is used to eliminate glial cells in mixed cultures [27] and as anti-tumor drug for cancer patients [28]. In conventional mixed neural cell cultures, AraC is applied for the first 24–48 hrs and removed by media change; however, such artificial drug removal cannot be readily extrapolated to *in vivo* drug clearance by cellular absorption and the brain's interstitial fluid flow [36]. Growing neural cells directly on drug-loaded silk films can better simulate the *in vivo* scenario at the close contact between drug reservoir and the brain tissue in order to evaluate the cell's response to on-target and continuous drug exposure. In our *in vitro* study, the significant extension of the efficacy threshold of AraC from 1 μM in solution to 16 μM in the silk fibroin films and of the toxicity threshold from 4 μM in solution to 32 μM in films suggest that cell response has different pharmacokinetics to substrate-bound drugs than to drugs in solution. A feedback loop by cell metabolism of drug molecules at the film interface due to physical proximity may contribute to dose-independent responses: Above a certain concentration, cell metabolites of AraC (ara-U) may attenuate further catabolism of excess drug, as observed in cancer patients treated with high-dose AraC [28,29]. With respect to drug toxicity, prolonged exposure time significantly increased toxicity of low-dose AraC in solution, but did not have significant effect on silk film-supported cultures of similar drug doses. These results can be explained by the lower mobility of substrate-bound drugs than in solution, as a result of which the cell's accumulative exposure would be less acute to film-released drugs than drugs in solution. These findings suggest that the silk film as drug carrier can increase the bioavailability but does not necessarily increase toxicity to adjacent cells. This feature would be desirable for central nervous system disorders that tolerate drug doses but require site specificity. For example, for the treatment of brain tumors, the silk film system can deliver high dose anti-cancer drugs to eliminate any residual tumor cells after incomplete tumor resection but spare the cells in the adjacent normal tissue.

4.2. Local drug delivery in an intact brain

Our *in vivo* studies provided direct evidence of small molecules passing through the dura of an intact brain and diffusing into the brain cortex. This delivery route allowed a negatively charged molecule, Evans blue, to diffuse despite previous reports suggesting that blood-brain barrier damage is required for passage into the brain parenchyma [30]. The present study has also identified additional small molecules that pass through an intact dura, including Hoechst, PI, and necrostatin. These findings indicate that the dura mater may be a more permissive barrier than the BBB, given its low cell density, few cell junctions and collagenous compositions [37].

The Evans blue study showed drug access to the mouse hippocampus within <72 hr after film implant. The cortical diffusion and the reach to the hippocampus also showed region specificity; as only the regions directly underneath the film implant were involved, while the contralateral hemisphere was not impacted. This regional specificity cannot be achieved by systemic injection. Considering the importance of the hippocampus in memory and that the placement of the film implants on the intact brain caused no behavioral changes, this feature could be useful for future pharmaceutical modulation of this critical region. In addition, our data showed that Evans blue was mostly cleared from the cortex by 8 days after implant, perhaps by the interstitial bulk flow between CSF compartment and the brain parenchyma [36]. Future engineering strategies could utilize this mechanism and tailor the film designs by varying its composition, such as porosity, crystallinity and nanoparticle incorporation [38], to achieve regional specificity, deeper access in the brain, and control of drug release kinetics.

Silk films in the brain were shown to be non-inflammatory and well-tolerated by the host animal. Degradation studies were not performed due to the difficulty of detecting and retrieving the thin films after implantation. However, silk fibroin-based scaffolds degraded less than 10% after 4 weeks in the brain of rats [15], potentially due to brain-endogenous chymotrypsin-like proteases [39,40]. Regarding brain tissue response, we did not examine dura-specific cell reactions such as intracranial mast cell's release of vasoactive, inflammatory and nociceptive signals that could contribute to migraines [41]. Nevertheless, with regard to neuroinflammation, there was no evidence of astrocyte or microglial activation or cell death in response to the presence of the films on intact dura. Even without the dura, the film presence caused no detectable behavioral or functional changes of the host animal. These features suggest that the silk film as drug carrier would not interfere drug actions in the brain.

4.3. Local drug delivery in injured brain

In injured brains such as in TBI, tissue damage, brain edema, and poor cerebral blood flow may significantly limit drug diffusion into the core of the brain lesion, in addition to the BBB [42,43]. To bypass the BBB, pre-clinical animal models are often administered test drugs via the intracerebroventricular route, by direct cannulation with a penetrating needle into the lateral ventricle [18,44]. This method ensures brain-wide access of drugs via the bulk flow of the CSF, yet at the expense of potential off-target toxicity. Our study demonstrates that silk fibroin film implants as an alternative route that is less invasive, more flexible and tunable to specific needs, and easier to use. We showed that topically applied silk films allowed drug diffusion directly into the lesion core of brain damage.

To compare silk film-based delivery with systemic delivery route, we used reciprocal delivery of PI and YOYO-1. Both are small molecules that can be indiscriminately taken up by cells with impaired membranes (necrosis), as indicated in the mixed film delivery result. However, when the two markers were co-delivered via different routes, one by film delivery and the other by IV injection, the markers were preferentially distributed either in the lesion core or the peri-lesional regions. The almost complementary pattern of marker distribution corresponded to film-based delivery (lesion core) versus IV injection (peri-lesional),

respectively. Figure 5 indicates that the total necrotic cell counts were comparable between different delivery routes of PI; whereas Figure 6 indicates that for the lesion *core* (not including peri-lesional area) there were more necrotic cells stained by film-delivered markers than IV injection. The differences between total versus core cell counts also imply that markers by IV injection had more access in the peri-lesional region. Together, these results provided evidence of a restrictive zone around the lesion border that limits marker passage across from either the lesion core (by film delivery) or from the systemic flow (by IV injection), as suggested by collapsed micro-vessels surrounding brain injury [42]. These findings imply that despite BBB damage resulting in drug access to the injured brain, blood flow-dependent delivery may still be partially excluded from the lesion core of brain damage. Therefore, the on-site film delivery would be particularly useful for injuries involving localized brain regions such as those encountered in TBI, brain tumors and focal epilepsy.

4.4 Silk film for drug testing in the brain

Finally, a pre-clinical drug application showed 40% reduction of acute cell injury after TBI by silk fibroin film-based necrostatin delivery. Necrostatin has been previously shown to reduce ~25% cell necrosis in the same CCI model [18]. However, due to instability of necrostatin in the blood (<60 min), previous studies of drug evaluation injected drug solution directly into the lateral ventricle. This study presented direct evidence of cell access and on-target effect of necrostatin that was comparable, if not better than previous studies; however, direct comparison of the two modes of delivery was not performed, nor was comprehensive outcome analysis including brain function with necrostatin treatment by film delivery. This study used a pre-treatment paradigm to confirm the short-term neuroprotection effect of necrostatin but not as a post-injury treatment. Previous studies have determined the short therapeutic window of intraventricularly-delivered necrostatin to be within 15 min after injury, reflecting the rapid acute injury phase (membrane damage, TNF alpha and Fas receptor induction) initiated in minutes after CCI as well as the immediate need to combat necrosis [18]. These disease studies underscore the complex sequalae of TBI's pathological progression and the importance of delivering therapeutics to appropriate biological targets. Therefore, a film as drug carrier with on-target delivery to regions of interest can be used to screen for drugs with neuroprotection effects with efficient validation of on-target cell response.

4.5 Implications for material choice and design for therapeutics delivery to the brain

Currently, Alzet™ pump delivery of compounds to the brain via cerebral ventricles or direct parenchymal infusion is the standard for targeted brain drug delivery; however, implantation of the device requires invasive surgery, causing cell and tissue death around the insertion site as well as increased risk of infection from the external minipumps. Many materials have been studied as tissue-engineered scaffolds or drug depots, including copolymers of polylactic acid and polyglycolic acid, deblock co-peptide polymers, alginates, chitin derivatives, and biocomposites [45]; many of which rely on a brain lesion such as an infarct, or require surgically induced lesions such as a needle tract. Some studies have used antibiotic-coated space-filling materials for restorative brain surgery [46]. Many of these materials have limited biocompatibility with the brain tissue as the material itself or its

degradation products may activate neuroinflammation or foreign body response that leads to glial scar encapsulation of the implant [47]; and materials derived from brain-enriched polymers such as hyaluronan hydrogel is being actively studied [48,49]. For drug delivery, extending release kinetics of therapeutics is a key area for improvement in material design such as multi-layer thin films [33]. Approaches of combining genetically engineered therapeutics-releasing cells or stem cells and encapsulating biomaterials are being tested for sustained release [50] as well as for host-graft integration and brain tissue regeneration [48,49,51,52]. The combination of the silk film's structural stability, conformal contact with the brain surface and compatibility with therapeutics incorporation and neural cell culture has motivated us to explore its use to support neuron-electrode interfaces for functional modulation of the brain [6]. This study further extends the utility of the silk film to include drug delivery for evaluating drug actions in normal and injured brains. Our ultimate goal is to use silk fibroin film or materials of similar functions to test a wide range of neuromodulation approaches (i.e., drug delivery, electrical stimulation, cell graft) in a live brain for comprehensive analysis of treatment outcomes, including cell responses and brain function. As the study has demonstrated, properties of the tissue-material interface and bulk tissue diffusivity may ultimately determine the outcomes of drug delivery in the brain; and disease-associated tissue property changes cannot be overlooked, such the constrictive border of a TBI lesion or altered interstitial fluid flow by brain tumor [53]. Therefore, the approach of combining *in vitro* cultures and *in vivo* testing with the same material and drug carrier format would be beneficial to distinguish biological outcomes, such as cell response, from material effects, such as pharmacokinetics.

5. Conclusions

Our studies showed that the silk fibroin films can be utilized to evaluate drug actions in both *in vitro* and *in vivo* studies of the brain with greater efficiency than existing approaches. In addition, the findings provided direct evidence of how different delivery routes reached cells via different mechanisms, especially in the injured brain. Though we did not have detailed analysis of behavioral or histological outcomes of the TBI model with film-delivered necrostatin, the ~40% reduction of cell necrosis is consistent with necrostatin's role in reducing histopathology and improvement of functional outcome as characterized in previous studies using intracerebroventricular delivery [18]. Finally, the demonstration of confined drug access by either on-site film delivery or IV injection, i.e., preferential to the lesion core or the peri-lesional area, respectively, in the brain lesion has broad implications for evaluating other drugs. These studies, however, have not shown *direct* comparison of a *same* drug in both *in vitro* cultures and *in vivo* brain studies with the film system. Only after establishing such feasibility of *in vitro*-to-*in vivo* translation of drug studies for a specific brain disorder, can the film system realize its potential as a better drug testing system than exiting options. Additionally, further development of the film system may include: simultaneous evaluation of drug effects with cell type-specific *in vitro* cultures and compare with tissue responses in a live brain, incorporation of multiple drugs in one film to test multiple compounds at once or cocktails of protective agents targeting more than one pathway, or grafting *in vitro*-optimized cells such as purified neurons into the brain with or

without neuron-electrode interfaces [6,8] to test for cell-based therapies or neuromodulatory interventions.

Acknowledgments

This work was funded by NIH (R01NS092847, R01NS094218, and EB002520) to D.L.K, 5RO1NS061255 to M. J. W., and Connecticut Children's Medical Center Strategic Research Fund and the Connecticut Institute of Brain and Cognitive Sciences (IBACS) Seed Grant 024 to M.D.T.

References

[1]. Hurko O, Ryan JL. Translational research in central nervous system drug discovery. NeuroRx 2005;2:671–682. [PubMed: 16489374]

[2]. Tang-Schomer MD, White JD, Tien LW, Schmitt LI, Valentin TM, Graziano DJ, Hopkins AM, Omenetto FG, Haydon PG, Kaplan DL. Bioengineered functional brain-like cortical tissue. Proc Natl Acad Sci U S A 2014;111:13811–13816. [PubMed: 25114234]

[3]. Iwashita M, Kataoka N, Toida K, Kosodo Y. Systematic profiling of spatiotemporal tissue and cellular stiffness in the developing brain. Development 2014;141:3793–3798. [PubMed: 25249464]

[4]. Tien LW, Wu F, Tang-Schomer MD, Yoon E, Omenetto FG, Kaplan DL. Silk as a Multifunctional Biomaterial Substrate for Reduced Glial Scarring around Brain-Penetrating Electrodes. Adv Func Mater 2013;23:3185–3193.

[5]. Kim DH, Viventi J, Amsden JJ, Xiao J, Vigeland L, Kim YS, Blanco JA, Panilaitis B, Frechette ES, Contreras D, Kaplan DL, Omenetto FG, Huang Y, Hwang KC, Zakin MR, Litt B, Rogers JA. Dissolvable films of silk fibroin for ultrathin conformal bio-integrated electronics. Nat Mater 2010;9:511–517. [PubMed: 20400953]

[6]. Tang-Schomer MD, Hu X, Hronik-Tupaj M, Tien LW, Whalen MJ, Omenetto FG, Kaplan DL. Film-Based Implants for Supporting Neuron-Electrode Integrated Interfaces for The Brain. Adv Func Mater 2014;24:1938–1948.

[7]. White JD, Wang S, Weiss AS, Kaplan DL. Silk-tropoelastin protein films for nerve guidance. Acta Biomater 2015;14:1–10. [PubMed: 25481743]

[8]. Hronik-Tupaj M, Raja WK, Tang-Schomer M, Omenetto FG, Kaplan DL. Neural responses to electrical stimulation on patterned silk films. J Biomed Mater Res 2013;101A:2559–2572.

[9]. Jin H, Park J, Karageorgiou V, Kim U, Valluzzi R, Cebe P, Kaplan D. Water-stable silk films with reduced beta-sheet content. Adv Func Mater 2005;15:1241–1247.

[10]. Hu X, Shmelev K, Sun L, Gil E, Park S, Cebe P, Kaplan D. Regulation of Silk Material Structure by Temperature-Controlled Water Vapor Annealing. Biomacromolecules 2011;12:1686–1696. [PubMed: 21425769]

[11]. Pritchard EM, Dennis PB, Omenetto F, Naik RR, Kaplan DL. Review physical and chemical aspects of stabilization of compounds in silk. Biopolymers 2012;97:479–498. [PubMed: 22270942]

[12]. Pritchard EM, Kaplan DL. Silk fibroin biomaterials for controlled release drug delivery. Expert Opin Drug Deliv 2011;8:797–811. [PubMed: 21453189]

[13]. Hines DJ, Kaplan DL. Mechanisms of controlled release from silk fibroin films. Biomacromolecules 2011;12:804–812. [PubMed: 21250666]

[14]. Wilz A, Pritchard EM, Li T, Lan JQ, Kaplan DL, Boison D. Silk polymer-based adenosine release: therapeutic potential for epilepsy. Biomaterials 2008;29:3609–3616. [PubMed: 18514814]

[15]. Szybala C, Pritchard EM, Lusardi TA, Li T, Wilz A, Kaplan DL, Boison D. Antiepileptic effects of silk-polymer based adenosine release in kindled rats. Exp Neurol 2009;219:126–135. [PubMed: 19460372]

[16]. Pritchard EM, Szybala C, Boison D, Kaplan DL. Silk fibroin encapsulated powder reservoirs for sustained release of adenosine. J Control Release 2010;144:159–167. [PubMed: 20138938]

[17]. Whalen MJ, Dalkara T, You Z, Qiu J, Bermpohl D, Mehta N, Suter B, Bhide PG, Lo EH, Ericsson M, Moskowitz MA. Acute plasmalemma permeability and protracted clearance of injured cells after controlled cortical impact in mice. J Cereb Blood Flow Metab 2008;28:490–505. [PubMed: 17713463]

[18]. You Z, Savitz SI, Yang J, Degterev A, Yuan J, Cuny GD, Moskowitz MA, Whalen MJ. Necrostatin-1 reduces histopathology and improves functional outcome after controlled cortical impact in mice. J Cereb Blood Flow Metab 2008;28:1564–1573. [PubMed: 18493258]

[19]. Lawrence BD, Marchant JK, Pindrus MA, Omenetto FG, Kaplan DL. Silk film biomaterials for cornea tissue engineering. Biomaterials 2009;30:1299–1308. [PubMed: 19059642]

[20]. Benfenati V, Toffanin S, Capelli R, Camassa LM, Ferroni S, Kaplan DL, Omenetto FG, Muccini M, Zamboni R. A silk platform that enables electrophysiology and targeted drug delivery in brain astroglial cells. Biomaterials 2010;31:7883–7891. [PubMed: 20688390]

[21]. Lawrence BD, Pan Z, Weber MD, Kaplan DL, Rosenblatt MI. Silk film culture system for in vitro analysis and biomaterial design. J Vis Exp 2012;(62). pii: 3646. doi:10.3791/3646. [PubMed: 22565786]

[22]. Rockwood DN, Preda RC, Yucel T, Wang X, Lovett ML, Kaplan DL. Materials fabrication from Bombyx mori silk fibroin. Nat Protoc 2011;6:1612–1631. [PubMed: 21959241]

[23]. Degterev A, Huang Z, Boyce M, Li Y, Jagtap P, Mizushima N, Cuny GD, Mitchison TJ, Moskowitz MA, Yuan J. Chemical inhibitor of nonapoptotic cell death with therapeutic potential for ischemic brain injury. Nat Chem Biol 2005;1:112–119. [PubMed: 16408008]

[24]. Tang-Schomer MD, Patel AR, Baas PW, Smith DH. Mechanical breaking of microtubules in axons during dynamic stretch injury underlies delayed elasticity, microtubule disassembly, and axon degeneration. FASEB J 2010;24:1401–1410. [PubMed: 20019243]

[25]. Bermpohl D, You Z, Lo EH, Kim HH, Whalen MJ. TNF alpha and Fas mediate tissue damage and functional outcome after traumatic brain injury in mice. J Cereb Blood Flow Metab 2007;27:1806–1818. [PubMed: 17406655]

[26]. Gerlai R Behavioral tests of hippocampal function: simple paradigms complex problems. Behav Brain Res 2001;125:269–277. [PubMed: 11682118]

[27]. Devon RM Elimination of Cell Types from Mixed Neural Cell Cultures In: Protocols for Neural Cell Culture. : SpingerLink p 325–332.

[28]. Ho DH, Frei E 3rd. Clinical pharmacology of 1-beta-d-arabinofuranosyl cytosine. Clin Pharmacol Ther 1971;12:944–954. [PubMed: 5289712]

[29]. Capizzi RL, Yang JL, Cheng E, Bjornsson T, Sahasrabudhe D, Tan RS, Cheng YC. Alteration of the pharmacokinetics of high-dose ara-C by its metabolite, high ara-U in patients with acute leukemia. J Clin Oncol 1983;1:763–771. [PubMed: 6668493]

[30]. Ay I, Francis JW, Brown RH,Jr. VEGF increases blood-brain barrier permeability to Evans blue dye and tetanus toxin fragment C but not adeno-associated virus in ALS mice. Brain Res 2008;1234:198–205. [PubMed: 18725212]

[31]. Lawrence BD, Wharram S, Kluge JA, Leisk GG, Omenetto FG, Rosenblatt MI, Kaplan DL. Effect of hydration on silk film material properties. Macromol Biosci 2010;10:393–403. [PubMed: 20112237]

[32]. Huang X, Brazel CS. On the importance and mechanisms of burst release in matrix-controlled drug delivery systems. J Control Release 2001;73:121–136. [PubMed: 11516493]

[33]. Hsu BB, Park MH, Hagerman SR, Hammond PT. Multimonth controlled small molecule release from biodegradable thin films. Proc Natl Acad Sci U S A 2014;111:12175–12180. [PubMed: 25092310]

[34]. Gil ES, Mandal BB, Park SH, Marchant JK, Omenetto FG, Kaplan DL. Helicoidal multi-lamellar features of RGD-functionalized silk biomaterials for corneal tissue engineering. Biomaterials 2010;31:8953–8963. [PubMed: 20801503]

[35]. Hu X, Tang-Schomer MD, Huang W, Xia X, Weiss AS, Kaplan DL. Charge-Tunable Autoclaved Silk-Tropoelastin Protein Alloys That Control Neuron Cell Responses. Adv Func Mater 2013;23:3875–3884.

[36]. Iliff JJ, Wang M, Liao Y, Plogg BA, Peng W, Gundersen GA, Benveniste H, Vates GE, Deane R, Goldman SA, Nagelhus EA, Nedergaard M. A paravascular pathway facilitates CSF flow through

the brain parenchyma and the clearance of interstitial solutes, including amyloid beta. Sci Transl Med 2012;4:147ra111.

[37]. Vandenabeele F, Creemers J, Lambrichts I. Ultrastructure of the human spinal arachnoid mater and dura mater. J Anat 1996;189 (Pt 2):417–430. [PubMed: 8886963]

[38]. Wang X, Yucel T, Lu Q, Hu X, Kaplan DL. Silk nanospheres and microspheres from silk/pva blend films for drug delivery. Biomaterials 2010;31:1025–1035. [PubMed: 19945157]

[39]. Nelson RB, Siman R. Clipsin, a chymotrypsin-like protease in rat brain which is irreversibly inhibited by alpha-1-antichymotrypsin. J Biol Chem 1990;265:3836–3843. [PubMed: 2303481]

[40]. Nelson RB, Siman R, Iqbal MA, Potter H. Identification of a chymotrypsin-like mast cell protease in rat brain capable of generating the N-terminus of the Alzheimer amyloid beta-protein. J Neurochem 1993;61:567–577. [PubMed: 8336143]

[41]. Rozniecki JJ, Dimitriadou V, Lambracht-Hall M, Pang X, Theoharides TC. Morphological and functional demonstration of rat dura mater mast cell-neuron interactions in vitro and in vivo. Brain Res 1999;849:1–15. [PubMed: 10592282]

[42]. Schwarzmaier SM, Kim SW, Trabold R, Plesnila N. Temporal profile of thrombogenesis in the cerebral microcirculation after traumatic brain injury in mice. J Neurotrauma 2010;27:121–130. [PubMed: 19803784]

[43]. Lo EH, Singhal AB, Torchilin VP, Abbott NJ. Drug delivery to damaged brain. Brain Res Brain Res Rev 2001;38:140–148. [PubMed: 11750930]

[44]. Greenhalgh AD, Ogungbenro K, Rothwell NJ, Galea JP. Translational pharmacokinetics: challenges of an emerging approach to drug development in stroke. Expert Opin Drug Metab Toxicol 2011;7:681–695. [PubMed: 21521135]

[45]. Pakulska MM, Ballios BG, Shoichet MS. Injectable hydrogels for central nervous system therapy. Biomed Mater 2012;7:024101–6041/7/2/024101. Epub 2012 Mar 29.

[46]. Govender ST, Nathoo N, van Dellen JR. Evaluation of an antibiotic-impregnated shunt system for the treatment of hydrocephalus. J Neurosurg 2003;99:831–839. [PubMed: 14609161]

[47]. Fournier E, Passirani C, Montero-Menei CN, Benoit JP. Biocompatibility of implantable synthetic polymeric drug carriers: focus on brain biocompatibility. Biomaterials 2003;24:3311–3331. [PubMed: 12763459]

[48]. Cook DJ, Nguyen C, Chun HN, L Llorente I, Chiu AS, Machnicki M, Zarembinski TI, Carmichael ST. Hydrogel-delivered brain-derived neurotrophic factor promotes tissue repair and recovery after stroke. J Cereb Blood Flow Metab 2017;37:1030–1045. [PubMed: 27174996]

[49]. Moshayedi P, Nih LR, Llorente IL, Berg AR, Cinkornpumin J, Lowry WE, Segura T, Carmichael ST. Systematic optimization of an engineered hydrogel allows for selective control of human neural stem cell survival and differentiation after transplantation in the stroke brain. Biomaterials 2016;105:145–155. [PubMed: 27521617]

[50]. Li T, Ren G, Kaplan DL, Boison D. Human mesenchymal stem cell grafts engineered to release adenosine reduce chronic seizures in a mouse model of CA3-selective epileptogenesis. Epilepsy Res 2009;84:238–241. [PubMed: 19217263]

[51]. Bible E, Qutachi O, Chau DY, Alexander MR, Shakesheff KM, Modo M. Neo-vascularization of the stroke cavity by implantation of human neural stem cells on VEGF-releasing PLGA microparticles. Biomaterials 2012;33:7435–7446. [PubMed: 22818980]

[52]. Fernandez-Garcia L, Perez-Rigueiro J, Martinez-Murillo R, Panetsos F, Ramos M, Guinea GV, Gonzalez-Nieto D. Cortical Reshaping and Functional Recovery Induced by Silk Fibroin Hydrogels-Encapsulated Stem Cells Implanted in Stroke Animals. Front Cell Neurosci 2018;12:296. [PubMed: 30237762]

[53]. Kingsmore KM, Vaccari A, Abler D, Cui SX, Epstein FH, Rockne RC, Acton ST, Munson JM. MRI analysis to map interstitial flow in the brain tumor microenvironment. APL Bioeng 2018;2:10.1063/1.5023503. Epub 2018 Jun 26.

Statement of Significance

This study demonstrated that silk fibroin films can be used to evaluate drug actions both *in vitro* and *in vivo*, partially overcoming the significant delivery barriers of the brain. This system can be adapted for efficient drug access to specific brain regions and/or cell types. The film system can be further developed for testing a range of interventions with drugs, electrical signals or cell graft for analysis of treatment outcomes including cell responses and brain function.

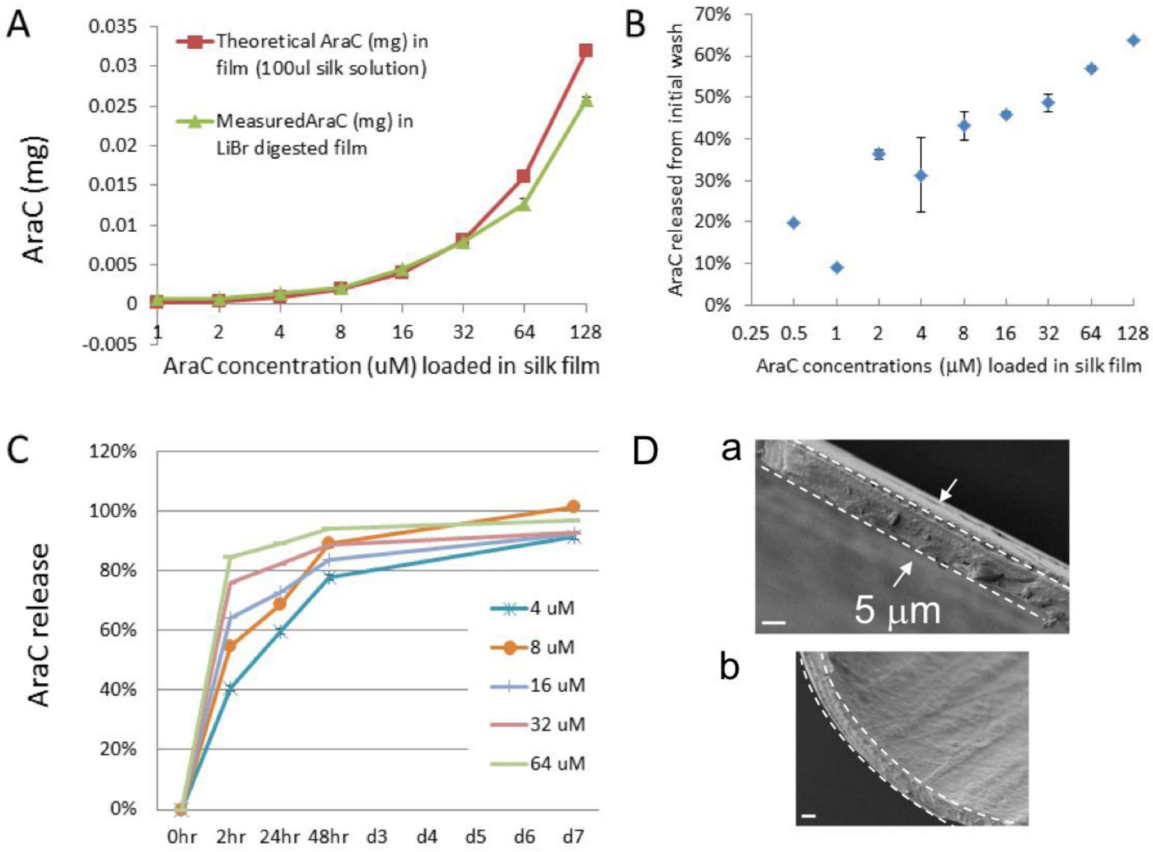

Figure 1: Release profile of arabinofuranosylcytidine (AraC) from silk films *in vitro*.

AraC content was measured with a spectrophotometer of absorbance at 272 nm. **(A)** Comparison of original loading doses (red line) with recovered AraC doses after dissolving silk films in LiBr (9.3 mL) (green line), indicating that most of loaded drugs were retained in silk films. **(B)** Percentage of AraC release during the step of poly-lysine coating of silk films, showing drug loss in proportion to the initial loading doses. This loss had been subtracted from the loading doses to reflect the actual retained amount of drug in silk films for cell culture studies (see Method). **(C)** Release profile of postprocessed AraC-silk films, showing a fast release within the first 2 hours and slower release up to days in vitro 7 (DIV7). (**D**) Scanning electron microscopic (SEM) images of silk films showing the cross-section (demarcated by the dashed lines in **a** & **b**) and the surface (**b**). Scale bar, 3 μm.

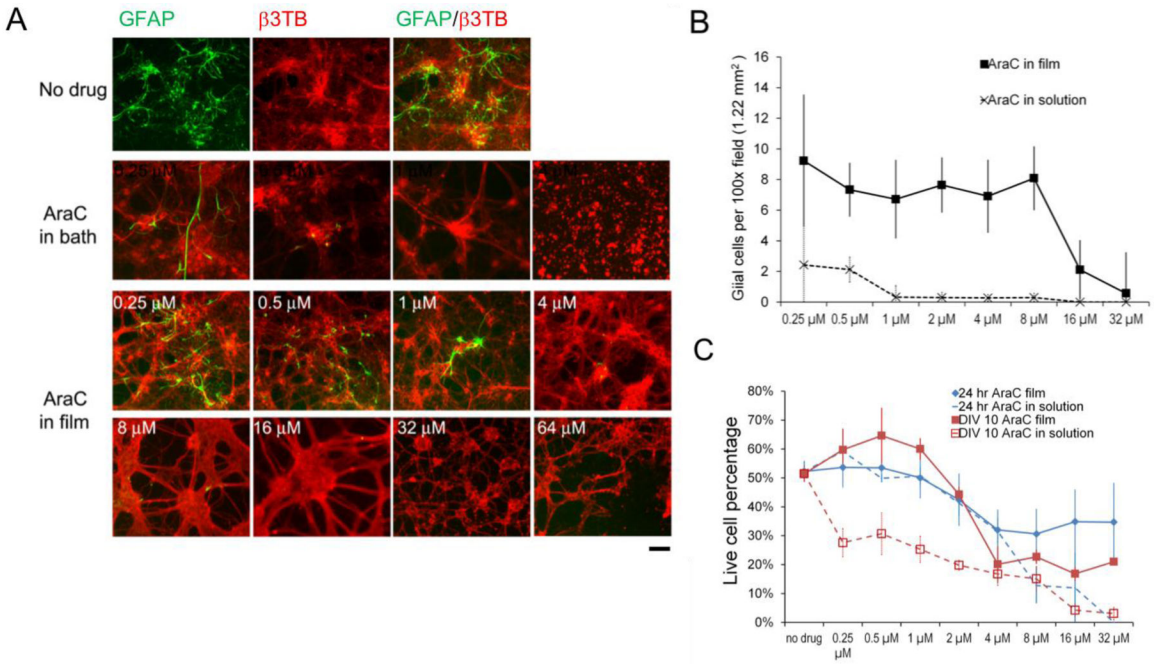

Figure 2. Primary rat cortical neural cells cultured on arabinofuranosylcytidine (AraC) -loaded silk films.

(**A**) Fluorescence photographs of DIV10 cortical mixed cultures co-stained with glial cell marker, GFAP (*green*) and neuronal marker, β III tubulin (β3TB) (*red*). AraC at higher concentrations (indicated in numbers) reduced GFAP-positive cells. Toxic levels of AraC (>64 μM) induced neuronal cell death and breaking of neuronal connections. Scale bar, 100 μm. (**B**) Quantification of GFAP+ cell counts (per 100× microscopic field of view of 1.22 cm^2) in DIV10 cultures on AraC in films (solid line), and with AraC in solution (dotted line). Error bar, standard error of mean (SEM), n = 3/group/time point. (**C**) Live cell percentages of cultures at 24hr with drug exposure (blue lines) and at DIV10 (red lines), on AraC in films (solid lines) and with AraC in solution (dotted lines). Error bar, SEM, n = 3/group/time point.

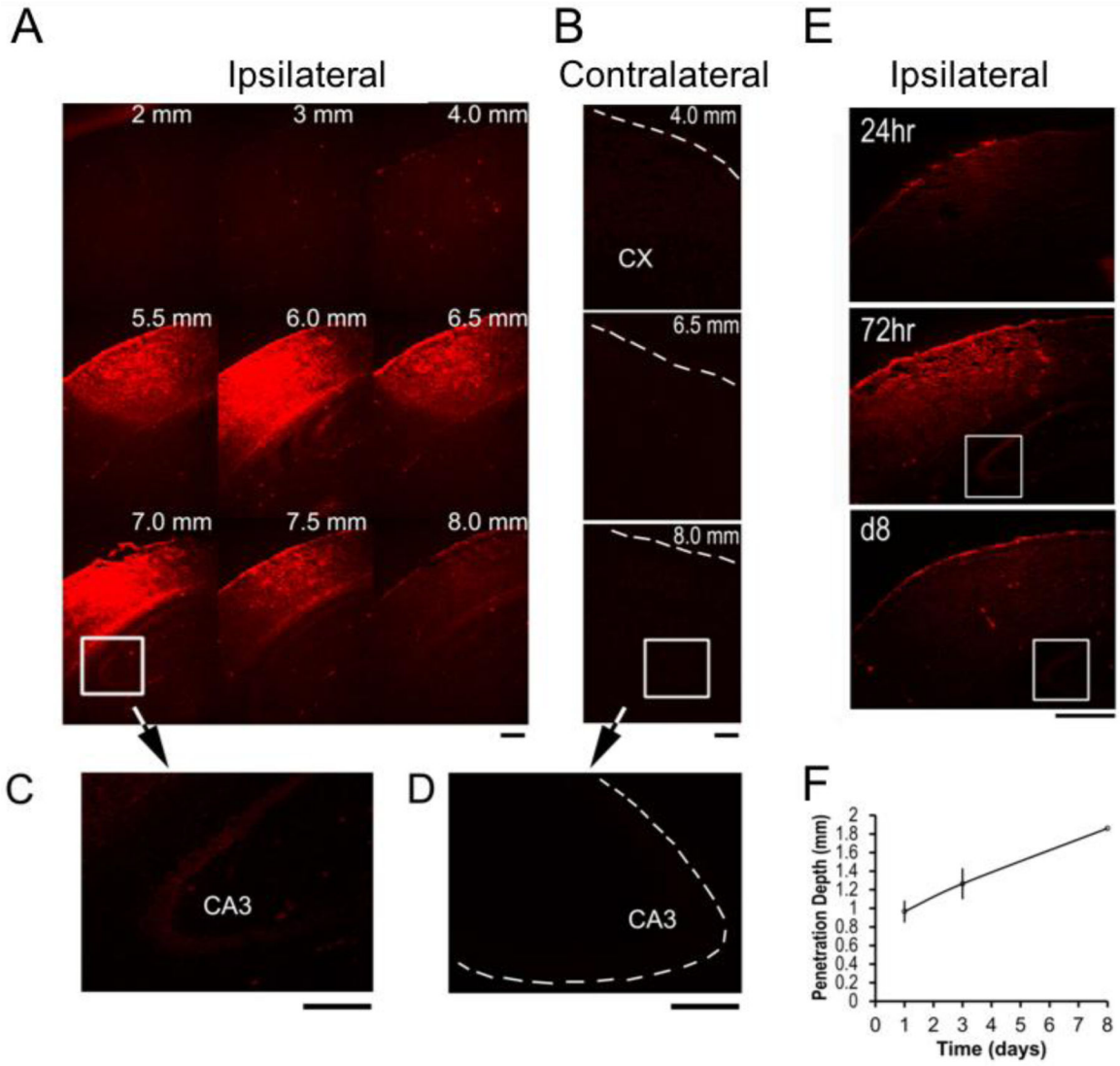

Figure 3. Silk film-based delivery of small molecules to localized cortical regions.

(**A**) By 72hr, Evans blue (EB, *red*) staining reached the maximum level and was detected in ipsilateral hippocampus CA3 region (white box). Numbers indicate the distance of the corresponding coronal section posterior to the olfactory bulb. Scale bar, 0.5 mm. (**B**) EB staining was negative in the contralateral hemisphere (dotted lines outline the cortical surface). Scale bar, 0.5 mm. (**C**) By 72hr, EB staining was detected in ipsilateral hippocampus CA3 region. The signal was weaker compared to the positive levels in the cortex after background normalization of the fluorescence signals. Scale bar, 0.5 mm. (**D**) EB staining was negative in the contralateral hippocampus CA3 region. Scale bar, 0.5 mm. (**E**) Time course of EB distribution in the ipsilateral hemisphere at 24hr, 72hr and day 8 (d8) post-implantation. The white box marks the hippocampus CA3 region. By d8, EB staining diminished to almost background levels. Scale bar, 0.5 mm. (**F**) Penetration depth of EB into the brain cortex, measured as the distance from the brain surface of the center of EB radial diffusion profile. The signal was considered positive when the staining intensity was at least 3× the level of the background staining. Error bar, SEM, n = 3/group/time point.

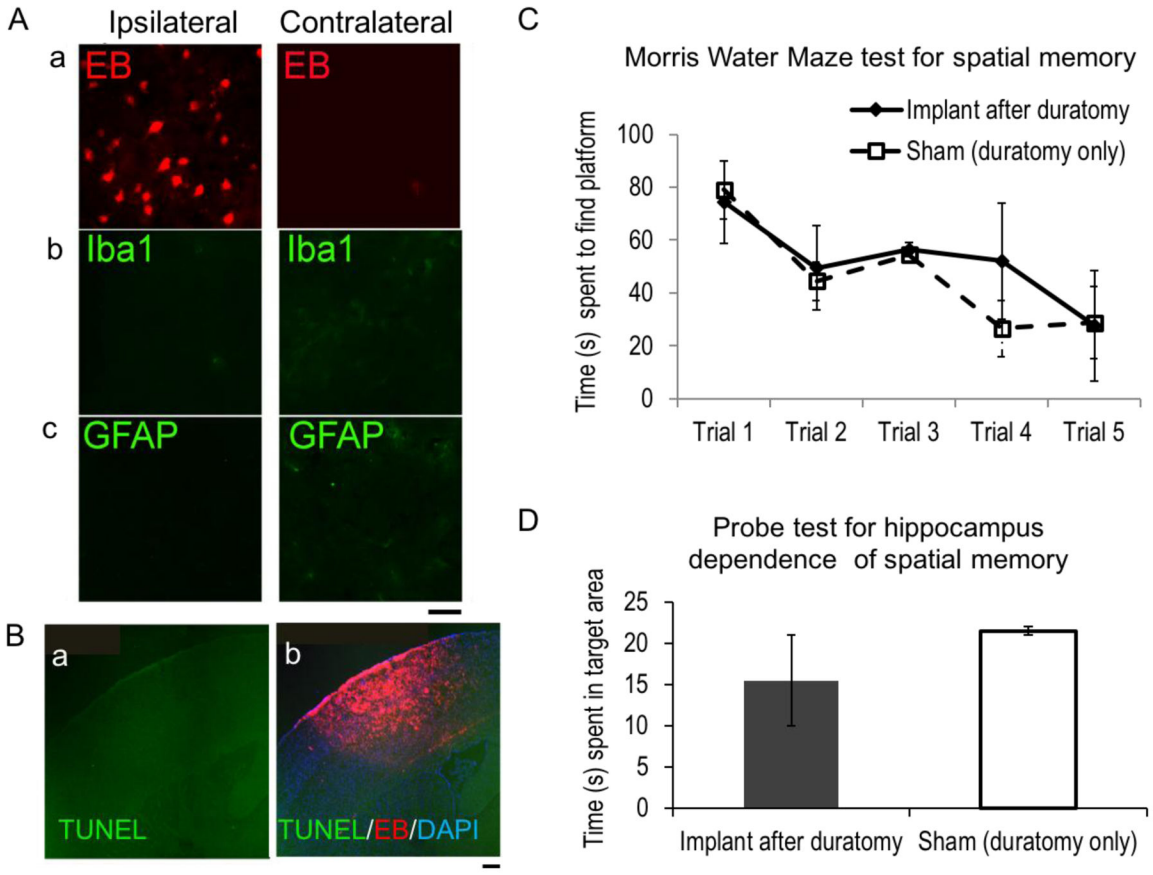

Figure 4. Brain tissue response to the presence of silk films and functional capacity.

(**A)** Representative coronal sections of mouse brains with EB-silk films at 3 days after implantation, stained for EB uptake (**a**), microglia marker, Iba1(**b**) and astrocyte marker, GFAP (**c**). The ipsilateral hemisphere (*left*) showed positive EB uptake, but not the contralateral hemisphere (*right*). Scale bar, 20 μm. (**B**) Representative TUNEL staining of coronal sections near the film implantation site (**a**) and overlaid with EB signals (*red*) and DAPI nuclei stain (*blue*) (**b**). Scale bar, 200 μm. (**C**) Morris Water Maze testing for spatial memory of mice with duratomy only (sham) and silk film implant (Implant after duratomy). (**D**) Probe test for hippocampus dependence of spatial memory of the same groups of mice as C.

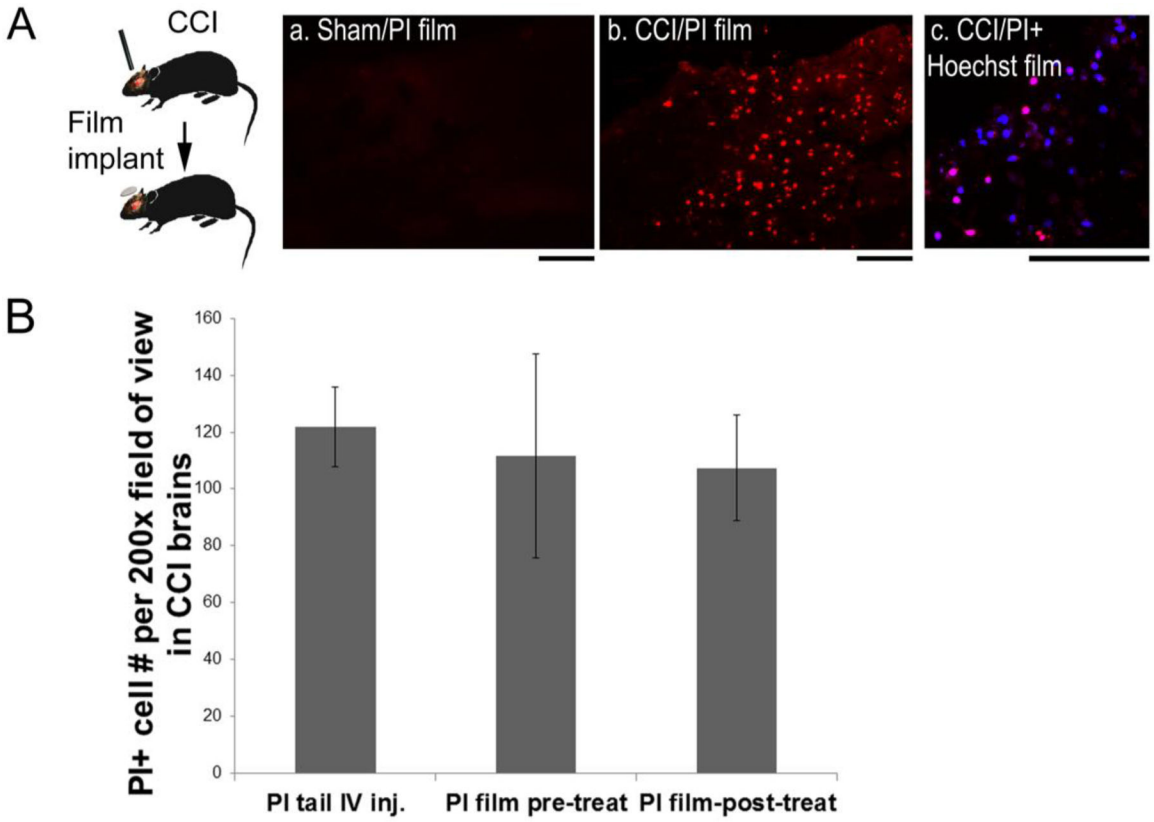

Figure 5. Silk film-based delivery of necrosis cell markers for labeling acute cell injury in a mouse TBI model.

(A) In a controlled cortical impact (CCI) mouse model, propidium iodide (PI)-encapsulated silk films were placed onto the exposed cortical surface immediately after CCI, and the brains were harvested at 5hr post-injury. (**B**) (**a**) No PI-positive cells were found in uninjured brains (sham) with PI films. (**b**) PI+ cells (*red*) were found in TBI brains with PI films. (**c**) Co-staining of PI (*red*) and Hoechst 33258 (*blue*) showed selectively injured cells (*pink*) in TBI brains with PI+Hoechst 33258 combined films. Scale bar, 100 μm. (**C**) Quantification of PI+ cells in contused cortex in mice after CCI. Animals were either pre-treated with PI-films for 24hr (pre-treat, n=4) or resided in the brain for 5hr after placement on top of the contusion site immediately after CCI (post-treat, n=8), and compared with those with conventional systemic PI injection (tail IV inj., n=8).

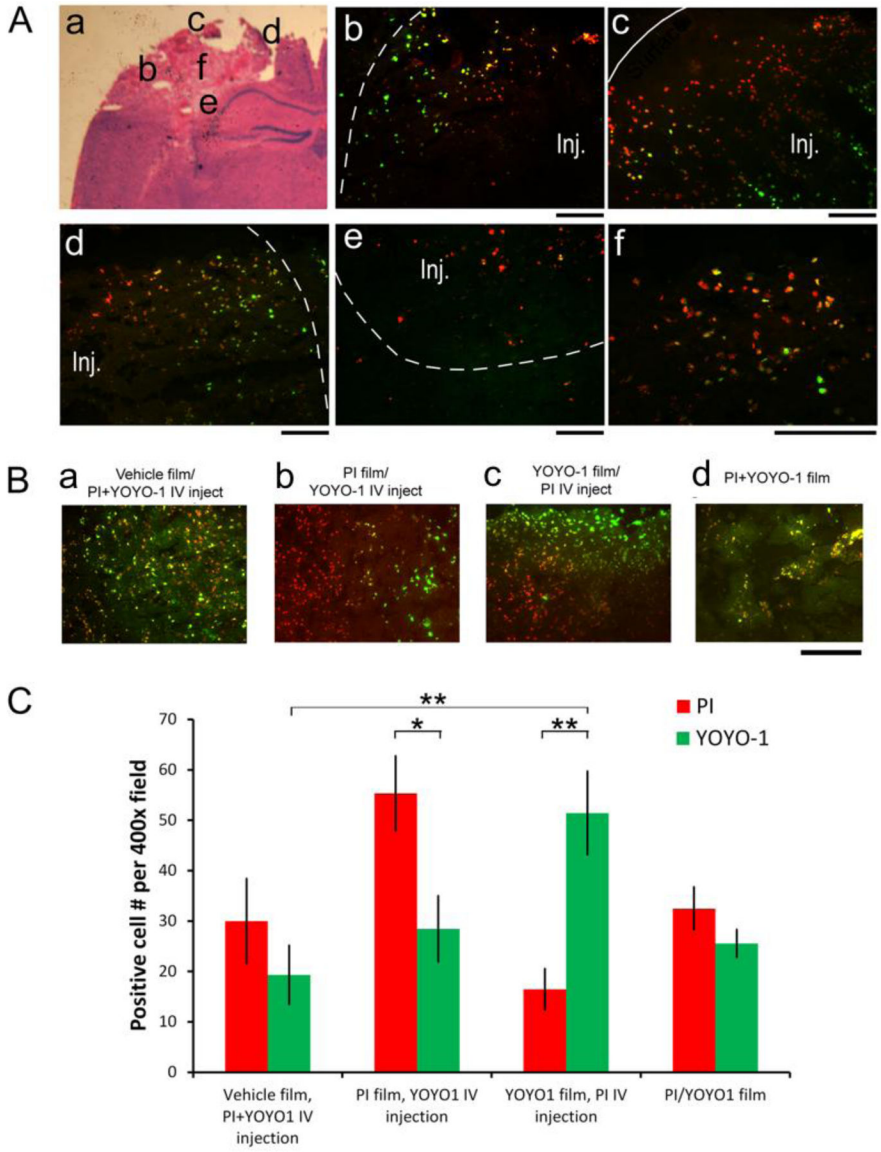

Figure 6. Silk Film-based delivery to overcome the restrictive peri-lesional zone of damaged brain tissue.

(**A**) Injured animals with PI films were administered with YOYO-1 via IV injection at 1hr post-injury, and the brains were harvested 30min later. Representative fluorescence photographs of injured brain sections schematized in **d,** showing the lateral (**e**), proximal (**f**), medial (**g**), inferior (**h**) regions surrounding the contusion (Inj., demarcated with dotted lines), and a higher magnification of the lesion center (**i**) (YOYO-1, *green*; PI, *red*). The edges of the contusion are demarcated with dotted lines, and the cortical surface with a solid line. Scale bar, 100 μm**. (B)** Representative fluorescence images of the lesion core of contused cortexes of mice with necrosis cell marker (PI, *red*, and YOYO-1, *green*) delivery. **(a)** Brain with vehicle films and PI and YOYO-1 combined IV injection. (**b**) Brains with PI films and YOYO-1 IV injection. (**c**) Brains with YOYO-1 films and PI IV injection. (**d**) Brains with PI and YOYO-1 combined films. Scale bar, 100 μm. **(C)** Quantification of PI+ (*red*) and YOYO-1+ (*green*) cell counts in the lesion core of brains with vehicle films plus PI

+YOYO-1 IV injection (n = 4), PI films with YOYO-1 IV injection (n = 6), YOYO-1 films with PI IV injection (n = 3), and PI/YOYO-1 combined films (n = 3) (Student's t-test, *, $p < 0.05$, **, $p < 0.01$).

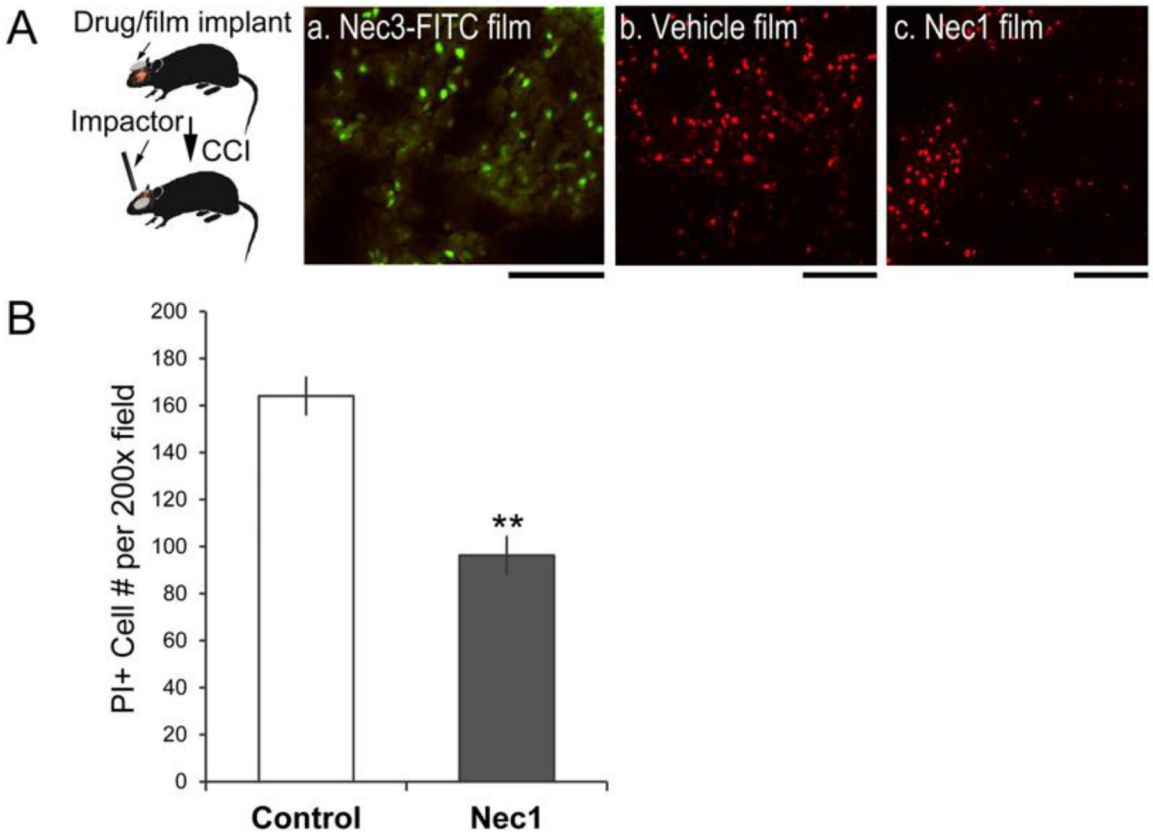

Figure 7. Silk film-based delivery of necrostatin for reducing acute cell injury in mouse brain after trauma.

(**A**) Necrostatin-encapsulated films were placed on brains at 24hr prior to injury and the brains were harvested at 5hr post-injury. (**a**) Fluorescently labeled necrostain 3 (Nec3-FITC) released from the film showed intracellular uptake in the injured cortex (*green*). (**b & c**) Systemic PI injection was used to label acutely injured cells at 5hr post TBI. Brains with vehicle films (**b**) had more PI+ cells than brains with Nec1 films (**c**). Scale bar, 100 μm. **(B)** Quantification of PI+ cell counts of injured brains with vehicle films and injured brains with Nec-1 films (n = 5/per group, Student's t-test, **, $p < 0.01$).